PERGAMON

International Journal of Heat and Mass Transfer 46 (2003) 1085–1095

International Journal of HEAT and MASS TRANSFER

www.elsevier.com/locate/ijhmt

Heat transfer studies during natural convection boiling in an internally heated annulus

M. Khalid Usmani [a,b], M. Altamush Siddiqui [a,*], S.S. Alam [a,d], A.M. Jairajpuri [a], M. Kamil [a,c]

[a] *Department of Mechanical Engineering, Aligarh Muslim University, Aligarh 202 002, India*
[b] *Department of Automobile Engineering, M.H. Saboo Siddik College of Engineering, Mumbai 400 008, India*
[c] *Department of Petroleum Studies, A.M.U., Aligarh 202 002, India*
[d] *Department of Chemical Engineering, A.M.U., Aligarh 202 002, India*

Received 27 December 1999; received in revised form 28 August 2002

Abstract

Heat transfer study has been carried out during natural convection boiling in an internally heated vertical annulus. The test section consists of a stainless steel tube, enclosed in a corning glass tube, forming an annular space through which the working fluid (water) flows. The S.S. tube is electrically heated. The experimental measurements have been made of wall temperatures along the length of the stainless steel tube and the inlet–outlet temperatures of the working fluid at the test-section, separator and condenser. Temperatures and mass flow rates of the cooling water entering and leaving the condenser, have also been recorded. The experiment was carried out for different heat fluxes impressed over the steel tube and repeated for two submergence levels of the liquid in the down flow pipe. Local and average heat transfer coefficients of the water film on the stainless steel tube surface, have been determined. Subsequently, the non dimensional parameters governing heat transfer and buoyancy induced flow processes, have been calculated and exhibited graphically. Correlations between the various parameters have also been developed.

1. Introduction

In recent years, considerable interest has been shown in the natural convection heat transfer to fluids in heated vertical open-ended annuli. Such systems are of practical importance in a variety of fields such as nuclear reactors, particularly the cooling of fuel elements during shut off periods. They may also be useful in solar heating and ventilating applications for domestic purposes [1]. A concentric annular duct is of great technical importance, as it is used in numerous heat transfer and fluid flow devices involving two fluids; one flowing through the inner tube, while the other through the annular passage between the two tubes. For example, gas cooled electrical cables require consideration of heat transfer in annular flow. Heat exchangers, evaporators and reboilers designed for chemical processes present additional examples where the results of buoyancy-induced convection in an annulus are useful [2]. Concentric annulus, apart from being a convenient heat exchange configuration, affords a simple model for replicating transport phenomena in rod-bundles [3].

El-Shaarawi and Sarhan [4] and Oosthuizen and Paul [5], studied analytically the free convective flow through a vertical open-ended annulus for isothermal heating. Information for a uniform heat flux surface were generated by Al-Arabi et al. [1]. Finite difference solution for two cases: (i) the inner rod being uniformly heated, with the outer shell adiabatic, and (ii) the outer wall being heated, while the inner rod kept adiabatic, have been presented in [4,6]. To support this analysis, they

* Corresponding author. Address: Department of Mechanical Engineering, Aligarh Muslim University, Aligarh 202 002, India. Tel.: +91-0571-702-247; fax: +91-0571-702-247.

E-mail address: altamushsiddiqui@yahoo.co.in (M. Altamush Siddiqui).

0017-9310/03/$ - see front matter
PII: S0017-9310(02)00368-X

Nomenclature

A_f	flow area (m^2)
C	specific heat (J/kg °C)
D_b	bubble diameter (m)
d_g	inner diameter of glass shell (m)
d_h	hydraulic diameter (m)
d_s	outer diameter of steel tube (m)
h_a	average heat transfer coefficient (W/m^2 °C)
h_{fg}	latent heat of vaporization (J/kg)
h_l	local heat transfer coefficient (W/m^2 °C)
k	thermal conductivity (W/m °C)
L	length of heated tube (m)
m	mass flow rate (kg/s)
q	heat flux (W/m^2)
S	submergence level (%)
T	temperature (°C)
Z	distance along the test section (m)

Greek symbols

α	thermal diffusivity (m^2/s)
ρ	density (kg/m^3)
μ	dynamic viscosity (Ns/m^2)
v	kinematic viscosity (m^2/s)
β	coefficient of thermal expansion (K^{-1})
σ	surface tension (N/m)
Δ	difference

Subscripts

b	boiling
c	condensate
i	Inlet
l	liquid
nb	non-boiling
o	outlet
s	saturation
sp	separator
v	vapour
wi	inlet cooling water to the condenser
wo	outlet cooling water to the condenser
1,2,-n	thermocouple number

Dimensionless groups

Convective Nusselt Number $Nu_c = hd_h/k_l$

Reynold's number for flow $Re = md_h/A_f\mu_l$, where $d_h = (d_g^2 - d_s^2)/d_s$ and $A_f = \pi(d_g^2 - d_s^2)/4$

Prandtl number $Pr = (\mu C/k)_l$

Grashoff number $Gr = g\rho_l^2 d_h^3 \beta \Delta T/\mu_l^2$

Nusselt number for boiling $Nu_b = hD_b/k_l$

Peclet number for boiling $Pe_b = qD_b/h_{fg}\alpha\rho_v$, where $D_b = \sqrt{\sigma/(\rho_l - \rho_v)g}$

also carried out experiments on a 1.67 m tall annulus with a heated rod of 12.2 mm O.D. and 47 mm I.D. shell, corresponding to a radius ratio of 0.26, using air as the fluid.

Numerical solutions for the induced flow and convection heat transfer, through a vertical annulus, has been obtained by Mohanty and Dubey [3] who considered the inner wall to be at uniform heat flux and the outer wall adiabatic, with air in the annulus. They have compared their results with experiments on a 3.68 m tall annulus of radius ratio 2.4. Both, the numerical and experimental results, cover higher flow ranges.

Andros and Florschuetz [7] visualized the flow patterns in an annular thermosiphon with a glass outer cylinder. For small and intermediate fills, four basic flow regimes were observed in the evaporator section for increasing heat load. The regimes were: (i) a smooth continuous film with surface evaporation, (ii) break down of the smooth continuous film into a series of stable rivulets, (iii) a wavy film with unstable rivulets, and (iv) a wavy film with bubble nucleation occurring in the unstable rivulets. At a very high heat input, on the other hand, complete dry out in the evaporator resulted. Lin et al. [8] experimentally studied the geyser boiling in a vertical annular two-phase closed thermosiphon. The effects of the heat load, condenser temperature, degree of liquid film and length of the evaporator on the characteristics of the geyser boiling were investigated in detail for both water and ethanol as working fluids.

However, the studies reported so far on thermosiphonic flow through annulli is confined either to air as the working fluid or geyser boiling. The data on closed loop thermosiphonic boiling in annulli is scarce. Keeping the above in view, the present study has been conducted to generate experimental data and investigate the effect of some important parameters such as heat flux and liquid submergence on heat transfer and induced flow during boiling of a liquid in an internally heated vertical annulus.

2. Experimental set-up

The experimental set up is essentially a closed loop circulation system consisting of a test section connected to a separator, condenser and a down flow pipe along with other accessories as shown schematically in Fig. 1. The geometrical configuration of the test section is an annulus made of two concentric tubes; the inner made of stainless steel while the outer of corning glass. The glass tube has dimensions of 45 mm inner and 48 mm outer diameters, with length equal to 1175 mm. The inner tube is of 32 mm I.D. and 38 mm O.D.; with effective length equal to 1000 mm and annular gap of around 3.5 mm.

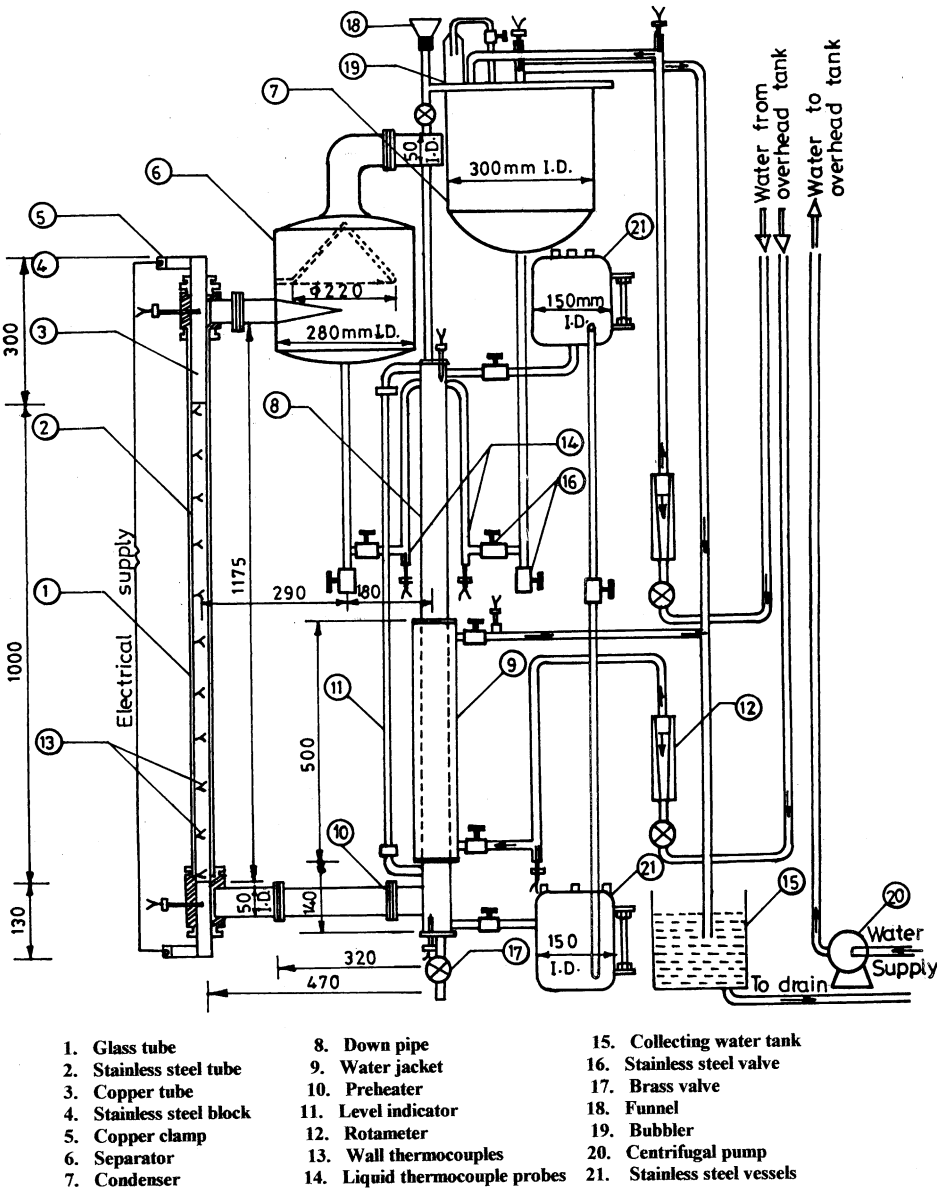

Fig. 1. Schematic diagram of the experimental set-up.

The inner tube is elongated at both ends by joining same diameter copper pipes of suitable lengths, which pass through stainless steel seats located at the top and bottom ends of the test section. For the purpose of electrical connections, copper clamps with negligible contact resistance are also provided at the ends of the inner tube. The test section is electrically isolated from rest of the set up by means of specially designed flanges made of teflon, fitted at the lower and the upper ends of the test section.

For heating the inner tube of the test section, stabilized power is supplied through a 30 kVA low voltage high current transformer. The electrical energy input to the test section is measured with the help of calibrated precision type voltmeter and ammeter. In order to monitor the heat transfer surface temperatures along the tube length, 12 copper–constantan thermocouples are held at suitable distances on inside of the inner tube as shown in Fig. 2, by means of leaf springs fixed on a wooden rod, which passes through the tube. Temperatures of the fluid at the inlet and the outlet of the test section, are measured by inserting thermocouples in the flow line. The exit end of the test section is connected to the separator using a 50 mm I.D. pipe. The separator is a cylindrically shaped vessel made of stainless steel. The

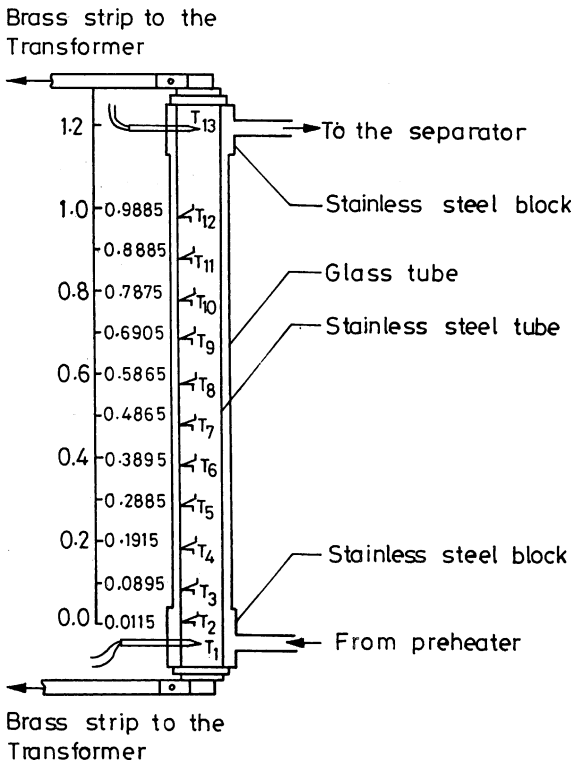

Fig. 2. Diagram showing thermocouple positions along the height in the test-section.

inner and the outer diameters of the vessel are 280 and 286 mm, respectively; the height of the vessel is 330 mm. The inlet line to the separator is connected tangentially. The liquid droplets, suspended in the vapor coming from the test-section, are separated by means of filter provided at the outlet of the separator. Temperature of the liquid, leaving the separator and entering the down flow pipe, is measured by a thermocouple inserted in this flow line.

The exit at the top end cover of the separator is connected to the condenser with the help of a 50 mm I.D. stainless steel pipe through which vapor leaving the separator passes. The condenser is also a cylindrical vessel with 300 mm I.D. and 350 mm height. A spiral coil of aluminum is fitted just below the top cover providing a surface for condensation. The cooling water for the spiral coil of the condenser is made available from the overhead tank provided at the top of the system. The flow of cooling water is regulated by means of a valve and measured using a rotameter. Provision is also made to detect complete condensation of the vapour coming from the separator. This is done by means of an inverted metallic U-tube fixed at the top of the condenser, the exit of which is immersed in a water filled bottle known as bubbler. The non-condensed vapour, if any, flows through this line and the bubbles escaping out can be seen in the bottle. If there is incomplete condensation, the excess vapour generation is controlled by increasing the cooling water flow rate. Temperatures of the cooling water at inlet and outlet of the condenser are measured using temperature probes inserted at appropriate positions in the flow line. Also, the temperature of the condensate leaving the condenser is measured using a thermocouple provided in the flowline from the condenser to the down flow pipe.

The liquid from the separator and the condensate from the condenser enter the downpipe at the top end; the separated liquid being at higher temperature than the condensate. The flow rate of the separated liquid and the condensate can be measured by collecting them for a fixed time through the valves provided in their respective flow lines as shown in Fig. 1. However, the valves in the main flow lines from the separator and the condenser to the inlet of the down flow pipe must be closed properly while measuring the flow rates of the separated liquid and the condensate. Temperature of the mixture at the inlet to the downpipe is measured using a thermocouple which is inserted facing downward in the cap at the top of the pipe. The down flow pipe in which the two liquid streams from the condenser and the separator meet, is jacketed with cooling water to regulate the inlet temperature of the liquid entering the test section. The height and the inner diameter of the cooling water jacket are 500 and 80 mm, respectively. The cooling water for this purpose is also taken from the overhead tank, the flow rate of which is measured by means of another liquid flowmeter. For the purpose of energy balance, temperatures of the cooling water entering and leaving the jacket are measured by two other thermocouples fixed at appropriate positions in the flow line of the coolant. Another thermocouple is also inserted through the cap, at the bottom of the cold leg, to measure the temperature of the liquid leaving the down flow pipe. A glass tube is provided along the cold leg to observe the liquid level in the down flow pipe. The maximum liquid head used in the present study corresponded to the liquid level equal to the top end of the annular test section. This condition has been termed 100% submergence [9–12]. Provision for charging of the fresh liquid is made by connecting a pipe, having a valve and a funnel, to the top end cap of the down flow pipe. At the bottom end cap of the down flow line, another pipe with a valve is provided for drainage of the liquid, whenever required.

3. Experimental procedure

After assembly, the experimental set up was tested hydraulically and ensured that there was no leakage at any point in the system. The entire set up was lagged with asbestos rope to reduce heat loss. The system was

then flushed with water to clean it thoroughly. The test section surface (stainless steel tube) was energized by adjusting an electrical input. The system was kept under operation for many hours followed by aging in order to obtain stable tube wall nucleating characteristics, which was essential for reproducibility of the data. A few runs were conducted to check the overall heat balance under the conditions of boiling. The water flow rates to the condenser and the jacketed down flow pipe were adjusted to give appreciable temperature rise. The readings of the electrical energy input, cooling water flow rates and all the thermocouples were taken when thermal equilibrium was established. Good agreement between the electrical energy supplied to the test section and heat energy removed in the condenser and the jacket ensured negligible heat losses from the set-up. Care was also taken that once the tube wall surface stabilized, it remained fully submerged with liquid as the dry test surface always entraps a very thin film of air. This air, on heating, takes the shape of tiny air bubbles which leave the surface on further heating and join the liquid. Thus, micro-convection sets in near the heat transfer surface in addition to the convection due to density differences. The additional turbulence so caused forms a major source of error and can be avoided by driving out the last traces of air from the system. Thus, for conducting a series of runs, the test liquid was boiled off for about 8–10 h to remove the last traces of dissolved air which was indicated by the disappearance of the air bubbles in the bubbler. Then a desired heat flux was impressed and the cooling water flow rates regulated to give maximum temperature rise consistent with no loss of vapour due to inadequate condensation. The liquid level in the down flow pipe was adjusted by either adding or draining the requisite amount of the test liquid. The unit was then operated for sufficient time to attain thermal equilibrium. When steady-state conditions were established, the readings were taken. The liquid level in the down flow pipe was observed and noted from the level indicator. The experimental data were generated at two different levels of liquid submergence (100% and 75%, varied independently) and heat fluxes ranging between 5 and 30 kW/m^2. Due to very small annular gap in the present set-up complete dry out resulted on the heating surface at high heat fluxes and low submergence levels.

4. Data reduction

The heat transfer surface temperature distribution along the length of the tube are obtained from the wall thermocouple readings after correction for the temperature difference across the wall thickness. In order to obtain the variation of test liquid temperature along the annulus height it is necessary to predict the non-boiling and boiling zones in the test section. Based on the thermal equilibrium model, as suggested by Saha and Zuber [13] and used by Kamil and Alam [9,10], effective lengths of the non-boiling and boiling zones were calculated. They can be obtained from the amount of net vapour generation and then condensation in the condenser. A heat balance around the condenser gives mass flow rate of the vapour into it as:

$$m_c = m_w C_{pw}(T_{wo} - T_{wi})/[h_{fg} + C_c(T_s - T_c)] \quad (1)$$

The effective boiling zone can now be determined by performing energy balance on the boiling zone of the test section, from the following equation:

$$Z_b = m_c h_{fg}/\pi d_s q \quad (2)$$

And the non-boiling zone,

$$Z_{nb} = L - Z_b \quad (3)$$

The liquid temperature distribution in the non-boiling zones of the test section was calculated from the following linear relationship,

$$T_l = T_{ll} + (T_s - T_{ll})Z/Z_{nb} \quad (4)$$

where $Z \leqslant Z_{nb}$.

The non-boiling zone as computed was almost the same as visualized experimentally through the glass tube. The wall and liquid temperatures in the test section, so obtained, have been plotted against the annulus height in Fig. 3 for the submergence level of 100% and 75% with different heat fluxes impressed on the tube. The wall temperatures rise steeply along the heated length of the tube from its inlet (lower) end up to points beyond which gradual fall sets in, showing maxima in each case. The wall temperatures then become almost constant in the remaining upper portion of the heated tube.

The liquid temperatures have been also plotted in (Fig. 3) showing temperature rise during sensible heating of the liquid, which subsequently become constant after attaining the saturation condition. The dashed line shows variation of the liquid temperature corresponding to the lowest heat flux. The region in the test section where sensible heating and subcooled boiling of the liquid takes place is characterized by the linear variation while the remaining top portion with almost constant temperature is the boiling zone. The location of the wall temperature peaks get shifted towards the test section inlet, as the liquid submergence is reduced and the heat flux increased.

The local heat transfer coefficients of the liquid film over the heated tube in the annulus-test section during closed loop natural convection boiling corresponding to the wall temperatures along the tube length are calculated from the following equation

$$h_l = q/(T_w - T_l) \quad (5)$$

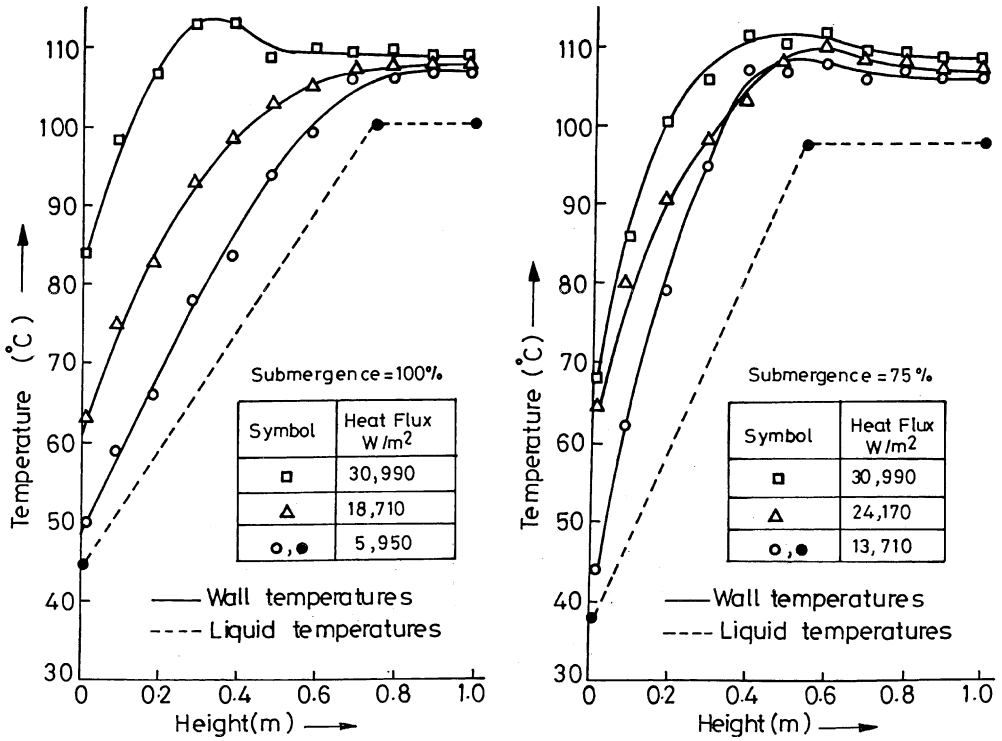

Fig. 3. Variation of the tube wall and liquid temperatures along the annulus height for different heat flux and submergence level.

Thus, for fixed heat flux on the heating surface and, $(T_w - T_l)$ evaluated for every thermocouple on the tube, h_l is calculated.

The average heat transfer coefficient for the test-section, at specified heat flux and submergence level, have been calculated from

$$h_a = q \Big/ \left[\sum_{i=2}^{12} (T_w - T_l)_i / 11 \right] \tag{6}$$

where $i = 2$–12, represent temperatures T_2 to T_{12} on the heated tube.

The rate of liquid circulation caused by buoyancy induced flow through the annular test section was evaluated by making a heat balance over the non-boiling zone [12], as follows:

$$q\pi d_s Z_{nb} = m_1 C_1 (T_s - T_{l1}) \tag{7}$$

so that,

$$m_1 = q\pi d_s Z_{nb} / C_1 (T_s - T_{l1}) \tag{8}$$

The circulation rate of the test liquid through the annulus were computed from Eq. (8) making use of the experimental data taken for the various operating conditions.

The heat transfer coefficients and induced circulation rates have been computed from the measured values of electrical input to the test section and various temperature at appropriate location with the help of thermocouples. The measurements involved include voltage, current, temperature and tube dimensions. The measured values are subjected to some uncertainties due to the error of measurement. Taking into account the least count and accuracy of each instrument employed, uncertainty analysis has been carried out using the method suggested by Kline and McClintock [14]. A numerical estimate of the uncertainty in heat transfer coefficient indicates that at the lowest heat flux 5.95 kW/m^2 and the lowest temperature difference of 4 °C, the maximum uncertainty is found to be ±12.82%. For all the other points of this heat flux, the uncertainty varies from ±5.8% to ±3.29%. At the highest heat flux of 30.99 kW/m^2, the maximum uncertainty is found to be 2.73%. The maximum uncertainty in the circulation rate is estimated to be ±2.32%.

5. Results and discussion

The values of local heat transfer coefficient as computed at various locations along the annulus height have been plotted for two submergence levels of 100% and 75% with heat flux as parameter in Fig. 4. The heat transfer coefficient decreases sharply from high values at

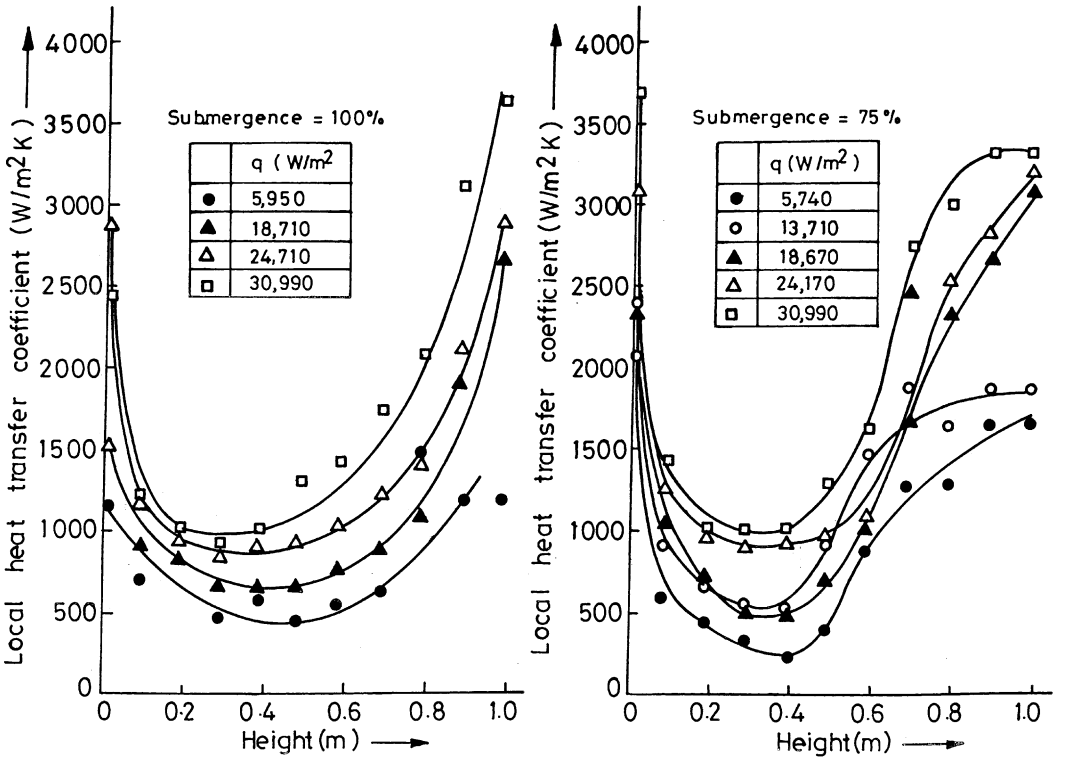

Fig. 4. Variation of the local heat transfer coefficient along the annulus height for different heat flux and submergence level.

the inlet end of the section, attain some minimum value and then start increasing at progressively enhancing rates. At 100% submergence and almost all the heat fluxes, the curves become very steep in the upper portion of the annulus. The initial decrease in the heat transfer coefficient may be due to the developing boundary layers in the entrance zone of the annulus. The increase in the values of heat transfer coefficient beyond certain heights may be attributed to the subcooled boiling. As the liquid moves upwards, the temperature rises and the boiling process gets intensified. Subsequently when the liquid temperature attains saturation value, the fully developed boiling sets in. This results in the net generation of vapour phase with the appearance of various flow patterns such as bubbly and slug flow regimes as shown in Plates 1 and 2. The steep rise in heat transfer coefficient is thus explained. The curves get shifted to higher values of transfer coefficients as the heat flux is raised, as expected. The nature of curves is quite similar even at the submergence level of 75%.

The variation of length average values of heat transfer coefficients with heat flux is shown in Fig. 5. The data are represented by almost linear parallel lines for the two submergences of 100% and 75%. The average heat transfer coefficient for 75% liquid is found to be higher than those for 100% submergence; probably due to the effective boiling setting in at a lower position in the former case as shown in Plates 3 and 4. This is due to the suppression of boiling by a higher circulation rate at 100% submergence than that at 75% submergence as observed in Fig. 7.

The average heat transfer coefficient in dimensionless form as Nusselt number has been plotted against the heat flux in non-dimensional form as Peclet number in Fig. 6.

The results shown in Figs. 5 and 6 are quite similar to each other and can be represented by the following equations:

$$h_a = 0.0394q + C_1; \quad [\text{for } 5 \leqslant q \leqslant 30.0 \text{ W/m}^2] \tag{9}$$

$$Nu_b = 0.0125Pe_b + C_2; \quad [\text{for } 50 \leqslant Pe_b \leqslant 400.0] \tag{10}$$

The values of constants C_1 and C_2 are given in Table 1.

The thermally induced flow of fluid through a vertical channel, tube/annulus, of a closed loop circulation system is established due to the differential head existing between the cold and hot legs. The hydrostatic head in the cold leg (down flow pipe) of the thermosiphonic system, depends upon the liquid submergence. The hydrostatic head in the hot leg (annular test section) is provided by the column of the test fluid whose quality

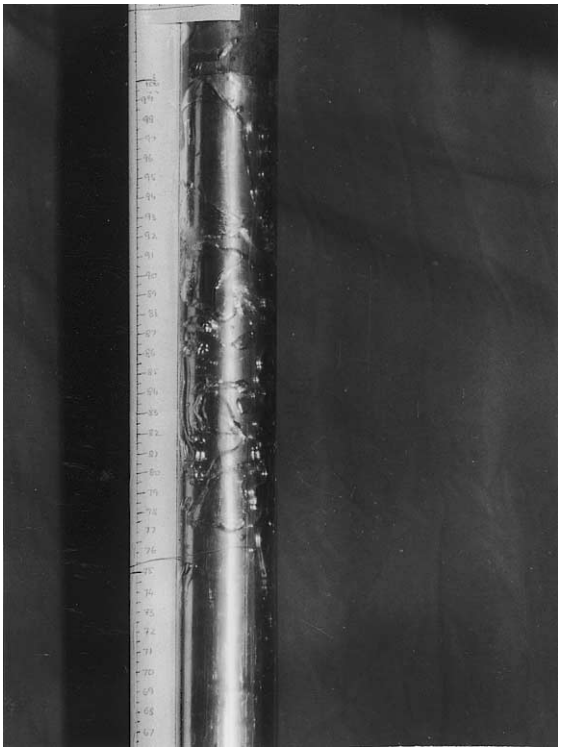

Plate 1. Bubbly and slug flow patterns at a heat flux of 13.7 kW/m^2 with 100% liquid submergence in the test section.

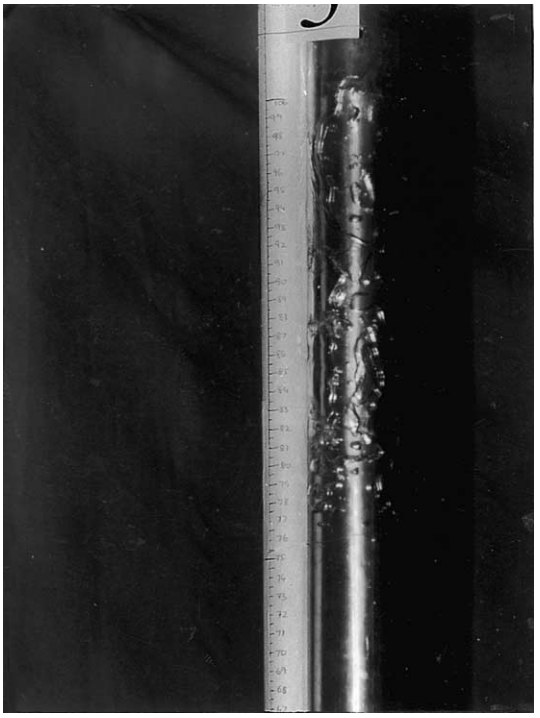

Plate 2. Bubbly and slug flow patterns at a heat flux of 18.71 kW/m^2 with 100% liquid submergence in the test section.

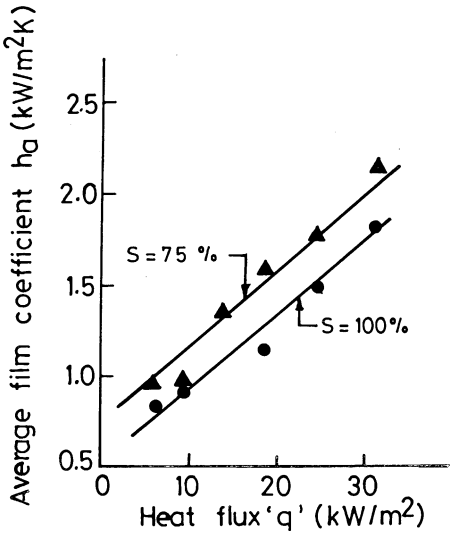

Fig. 5. Variation of the average heat transfer coefficient with heat flux.

Plate 3. Effective boiling zones at a heat flux of 9.5 kW/m^2 with $S = 100\%$ (left tube) and $S = 75\%$ (right tube).

changes with boiling and vapour generation as the fluid flows upwards. The rate of circulation, therefore, depends upon liquid submergence, heat flux, inlet liquid subcooling, vapour fraction and all those parameters which are involved in the frictional resistance of the circulation loop.

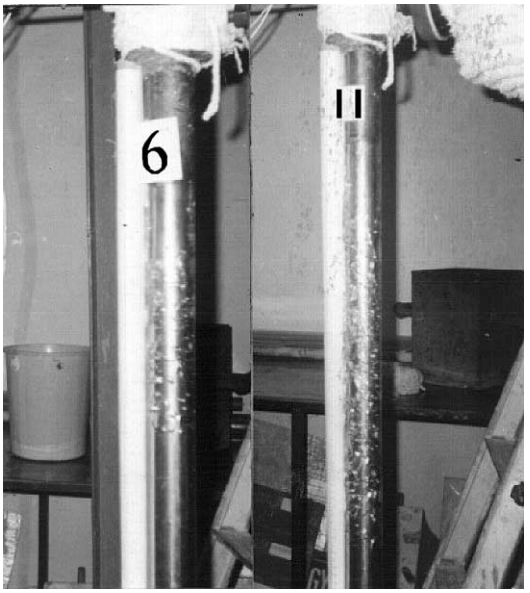

Plate 4. Effective boiling zones at a heat flux of 13.7 kW/m^2 with $S = 100\%$ (left tube) and $S = 75\%$ (right tube).

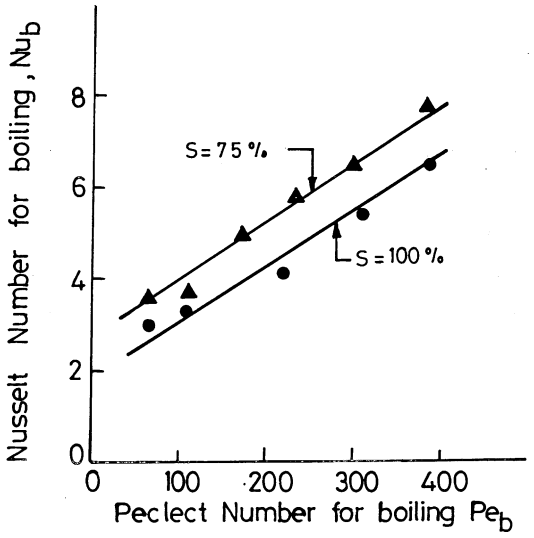

Fig. 6. Variation of the average Nusselt number with Peclet number.

The effect of heat flux on the circulation rate is shown in Fig. 7. The circulation rate is observed to increase from small values at a progressively increasing rate as the heat flux is raised from low to high values. Unlike the heat transfer coefficients, the circulation rate is higher for 100% submergence as compared to those when the submergence is 75%. Interestingly the curves for the two submergence levels deviate more and more from each other as the heat flux increases. At a given submergence, the liquid head in the cold leg remains the same while the increase in heat flux shifts the boiling incipience nearer to the heating surface-inlet and the saturated boiling occupies a longer length of the annulus resulting in the higher vapour fraction in the annular test section. The average density and hence the equivalent head of two-phase mixture gets reduced. Thus, the differential hydrostatic head responsible for fluid circulation increases with heat flux enhancing the flow rate, as observed in the Fig. 7. At a lower liquid submergence, the differential head becomes smaller than that at higher submergence despite the increase in vapour fraction due to more effective saturated boiling in the tube, thereby reducing the circulation rate at lower submergence.

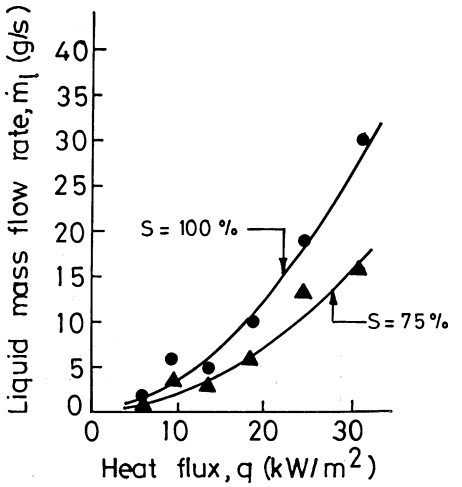

Fig. 7. Variation of the liquid flow rate (m_l) with heat flux number.

The variation of mass flow rate with heat flux has also been represented in terms of Reynold's number and Peclet number and found quite similar as shown in Fig. 8. However, the log-log plot of m_l versus q and Re versus Pe_b, as shown in Figs. 9 and 10, are found to be almost

Table 1
Constants C_1, C_2, C_3, C_4 and C_5 for the correlations

Submergence level (%)	C_1	C_2	C_3	C_4	C_5
100	550	1.9	8.1725×10^{-10}	0.242	29792.14
75	755	2.8	5.0575×10^{-10}	0.157	45116.35

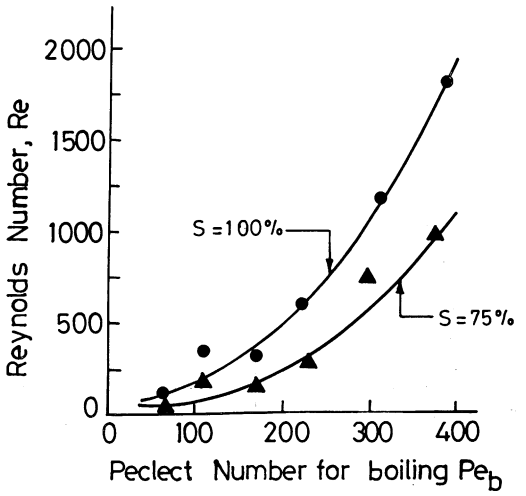

Fig. 8. Variation of Reynolds number with Peclet number.

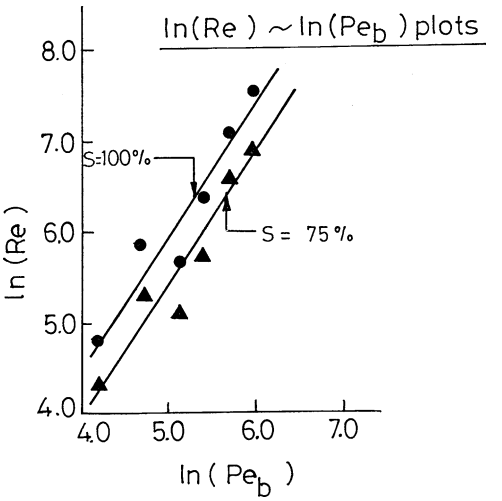

Fig. 10. Log–log plot of Reynolds number with Peclet number.

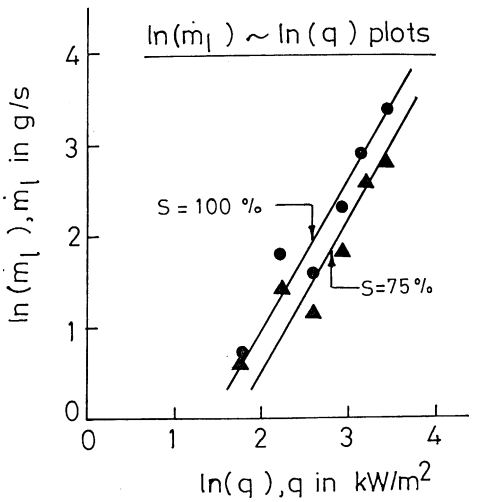

Fig. 9. Log–log plot of the liquid Reynolds flow rate (m_l) with heat flux.

parallel straight lines for the submergence levels of 100% and 75%. These may be represented by the following mathematical relations:

$$m_l = C_3 q^{1.686}; \quad [\text{for } 5 \leqslant q \leqslant 30.0,\ \text{kW/m}^2] \tag{11}$$

$$Re = C_4 Pe_b^{1.475}; \quad [\text{for } 50 \leqslant Pe_b \leqslant 400.0] \tag{12}$$

The constants C_3 and C_4 are given in Table 1.

From the preceding discussion on heat transfer and the resulting thermally induced flow in the thermosiphonic annulus, it is felt that there must exist a strong relationship between the two phenomena. In natural circulation loops, which are employed in a number of cooling applications, the free and forced convection effects obey the following functional form [15]:

$$Nu_c Gr/Pr = CRe^n \tag{13}$$

The dimensionless numbers, for the convective heat transfer, such as *Nu*, *Gr*, *Re* and *Pr* were computed for the experimental data and a correlation developed. The constant '*C*' and '*n*' so obtained, lead to the following general equation:

$$Nu_c Gr/Pr = C_5 Re^{0.673} \tag{14}$$

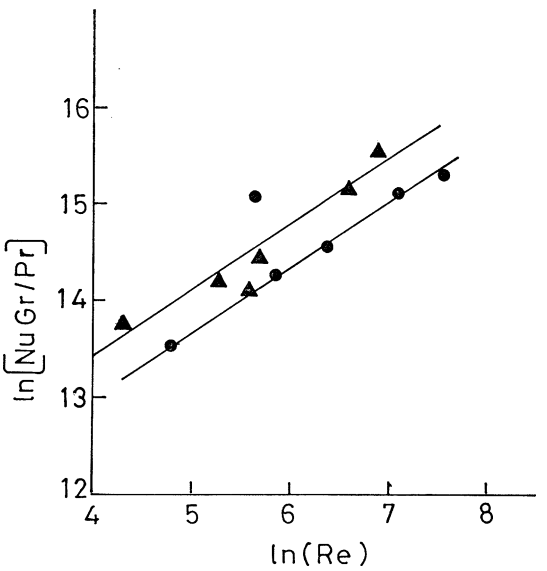

Fig. 11. Representation of the various dimensionless groups for the closed loop thermosiphonic system.

Table 2
Mean of the percentage deviation

Equations (%)	$Nu_b = 0.0125Pe_b + C_2$ (%)	$Re = C_4 Pe_b^{1.475}$ (%)	$Nu_c Gr/Pr = C_5 Re^{0.673}$ (%)
$S = 100$	+7	+4.6	−13
$S = 75$	+2.6	+20	−3

where, the values of C_5 for $S = 100\%$ and $S = 75\%$ are given in the Table 1.

A plot of $\ln[Nu_c Gr/Pr]$ versus $\ln[Re]$ has been presented in Fig. 11 for the submergence levels of 100% and 75%. Almost all the data points are found to be well represented by two straight lines resulting in (14). The range of numerical values of the parameters in Eq. (14) are $Nu_c = 14$–40, $Gr = 2.2 \times 10^5$–6×10^5, $Pr = 3.4$–4.8, and $Re = 50$–1670.

The properties of water in the test section were estimated at the inlet and outlet bulk temperatures, while those of the water-vapour at its saturation conditions.

Percentage deviation of the predicted values, using the proposed equations, from those obtained using the experimental results have been calculated for every set of the operating conditions. Except a few values, especially when $q = 13.7$ kW/m^2, which can also be seen in the respective plots, the percentage deviation lies within $\pm 20\%$. The mean values of all the deviations, calculated for each data are given in Table 2.

6. Conclusion

1. Variation in the local heat transfer coefficient through the annulus represents the developing boundary layer at the inlet end which is followed by subcooled boiling and then the fully developed boiling towards the exit.
2. The heat transfer coefficient and circulation rate increase with heat flux at a given level of submergence.
3. As the level of liquid submergence is lowered, the heat transfer coefficient gets enhanced while the circulation rate is reduced.
4. The mathematical relationships for Nusselt and Reynolds numbers with Peclet number are:

$$Nu_b = 0.0125Pe_b + C_2$$
$$Re = C_4 Pe_b^{1.475}$$

5. The heat transfer and the resulting thermally induced flow in the closed loop annulus are represented by

$$Nu_c Gr/Pr = C_5 Re^{0.673}$$

References

[1] M. Al-Arabi, M.A. El-Shaarawi, M. Khamis, Natural convection in uniformly heated vertical annuli, Int. J. Heat Mass Transfer 30 (1987) 1381–1389.

[2] N. Islam, Combined free and forced convection heat transfer in horizontal annulus, Ph.D. Thesis, Mechanical Engineering Department, IIT Bombay, 1997.

[3] A.K. Mohanty, M.R. Dubey, Buoyancy induced flow and heat transfer through a vertical annulus, Int. J. Heat Mass Transfer 39 (1996) 2087–2093.

[4] M.A. El-Shaarawi, A. Sarhan, Developing laminar free convection in a heated vertical open-ended annulus, Ind. Eng. Chem. Fundam. 20 (1981) 388–394.

[5] P.H. Oosthuizen, J.T. Paul, A numerical study of free convective flow through a vertical annular duct, ASME 86-WA/HT-81, Winter Annual Meeting, Anaheim, CA, 7–12 December, 1986.

[6] W. Elenbass, The dissipation of heat by free convection from the inner surface of vertical tubes of different shapes of cross-section, Phys. S' Grav. 9 (1942) 865–874.

[7] F.E. Andros, L.W. Florschuetz, The two phase closed thermosiphon: an experimental study with flow visualisation. In: Two Phase Transport and Reactor Safety, vol. 4, 1976, pp. 111–1239.

[8] T.F. Lin, W.T. Lin, Y.L. Tsay, J.C. Wu, Experimental investigation of geyser boiling in an annular two phase closed thermosiphon, Int. J. Heat Mass Transfer 38 (1995) 295–307.

[9] M. Kamil, S.S. Alam, H. Ali, Heat transfer to liquids in single vertical tube thermosiphon reboiler, Exp. Thermal Fluid Sci. 10 (1995) 44–53.

[10] M. Kamil, S.S. Alam, H. Ali, Predicting the onset of nucleate boiling in a vertical tube thermosiphon reboiler. In: M.D. Kellehar et al. (Ed.) Experimental Heat Transfer, Fluid Mechanics and Thermodynamics', vol. 2, Elsevier Science, Publishers B.V., New York, 1993, pp. 1232–1239.

[11] S.S. Alam, Boiling of liquids in vertical tubes, in: Heat and Mass Transfer '95, Tata McGraw-Hill, New Delhi, 1995, pp. 117–127.

[12] M. Kamil, S.S. Alam, H. Ali, Prediction of circulation rates in vertical tube thermosiphon reboiler, Int. J. Heat Mass Transfer 38 (4) (1995) 745–748.

[13] P. Saha, N. Zuber, An analytical study of the thermally induced two phase flow instabilities including the effect of thermal non-equilibrium, Int. J. Heat Mass Transfer 21 (1978) 415–426.

[14] S.J. Kline, F.A. McClintock, Describing uncertainities in single sample experiments, Mech. Eng. (1953) 3.

[15] J.P. Holman, in: Heat Transfer, McGraw-Hill International Book Company, New York, 1981, p. 295.